Case Study Comparison of the Seismic Performance of Reinforced Concrete and Concrete Filled Steel Tube Bridges

2017 NZSEE Conference

M.T. Stephens

Department of Civil and Environmental Engineering, University of Auckland, Auckland.

D.E. Lehman and C.W. Roeder

Department of Civil and Environmental Engineering, University of Washington, Seattle, Washington, USA.

ABSTRACT: Past earthquakes have resulted in significant damage to reinforced concrete (RC) highway bridge columns. Concrete filled steel tube (CFST) bridge columns have been introduced as an economical alternative to traditional RC columns, since they permit accelerated construction, reduce cost with smaller column diameter and material requirement, and superior inelastic seismic performance. To further explore the potential benefit of CFST bridges, a side-by-side comparison of the seismic performance of these two structural systems, RC and CFST, is made including damage and collapse potential using performance-based earthquake engineering (PBEE) tools. These tools include nonlinear analysis methods to capture the full cyclic inelastic response of the structural system, probabilistic-based functions to quantify the likelihood of damage and reparability, and incremental dynamic analyses (IDAs) to evaluate collapse potential. The comparison is made using a RC highway bridge in the US State of Washington as the case-study structure; the bridge was re-designed using CFST bridge columns with the objective of having the same stiffness and flexural strength. The RC and CFST structures were subjected to a suite of crustal ground motions scaled to represent serviceability (10% probability of exceedance in 50 years), design (7% probability of exceedance in 75 years), and maximum considered (2% probability of exceedance in 50 years) seismic hazard levels. Fragility curves were used to compare the performance of the structures in terms of damage state, and IDAs were used to compare damage and collapse potential. The results show that the CFST structure is more resilient than the RC structure by all measures.

1 INTRODUCTION

Highway bridges in seismic regions are commonly designed as moment resisting frames where the cap beams and foundations are capacity designed to resist the ultimate flexural resistance of the columns. Bridges are susceptible to damage and possible collapse when subjected to seismic loading, because the columns undergo inelastic deformations even at design level events. Guide specifications for reinforced concrete (RC) bridges typically require special detailing in regions of expected plastic hinging to increase deformation capacity and prevent hinge failure (AASHTO 2015; NZ Transport 2016). These detailing requirements typically result in congested reinforcing details which increase cost and the difficulty of construction.

Concrete filled steel tubes (CFST) columns are composite structural elements which are efficient and economical alternatives to conventional RC bridge columns. The steel tube acts as the formwork and reinforcing to the concrete fill, and the steel is at the optimal location for flexural resistance, thereby reducing the diameter of the column and weight and materials required for the column. Further, the steel tube provides greater confinement and shear strength to the concrete fill than transverse spiral reinforcement typically used for circular RC columns, while the concrete fill restrains local buckling of the steel tube. No reinforcement is required inside the tube, and this permits more economical and rapid placement of the concrete fill. CFSTs have larger compressive strength, stiffness and bending resistance

than RC column of the same weight and diameter, and they sustain less severe damage during earthquake deformations than RC columns (Lehman and Roeder 2012). As a result, CFSTs are a particularly attractive alternative to RC columns in seismic regions where bridge columns and connections are designed to resist inelastic reversed-cyclic loading.

Current code provisions governing the design of highway bridges in the US include expressions for establishing the strength and stiffness of CFST columns (AASHTO 2012), and recent research provides practical and straight-forward design expressions for CFST column-to-cap beam and column-to-foundation connections (Stephens et al. 2016a, 2016b). However, a side-by-side comparison of the performance of RC and CFST bridges including damage and collapse potential has not been made; to fully understand the benefits of CFST bridges in high seismic regions, a direct comparison, including quantification of repair required and collapse potential, of CFST and RC bridges are needed.

In this research, advanced performance based earthquake engineering (PBEE) tools are used to compare the seismic performance of a prototype bridge with RC and CFST columns. Fragility functions that express the likelihood of damage and reparability are used to estimate damage and repair requirements for the RC and CFST alternatives. Nonlinear analyses that simulate the full cyclic response of the structural systems are used to predict the seismic demand at specified hazard levels that quantify serviceability, design and maximum expected events. In addition, incremental dynamic analyses (IDAs) were conducted to estimate collapse resistance of each system.

2 CASE STUDY STRUCTURE

The Gold Creek Bridge (see Fig. 1) located near mile post 55 on Interstate 90 in Washington State was selected as the prototype bridge for this study. The bridge has seven 47.244m spans, and it was selected because the multiple spans limit the influence of the abutments on global response, and this permits more direct comparison of the alternate bridge column performance. The RC columns in the bridge were 1.524m in diameter, and required 18 No. 11 (~35mm diameter) longitudinal bars, and No. 6 spiral (~19mm diameter) with 76mm pitch in the transverse direction. The RC columns were re-designed as CFST columns with equivalent strength and effective stiffness under combined axial-moment (P-M) loading, which resulted in CFST columns 1.27 m and 16 mm in diameter and thickness, respectively, which results in a diameter to thickness ratio (D/t) of 80. The CFST cap beam and foundation connections were designed using an Embedded Ring (ER) connection in which an annular ring is welded to the end of the steel tube and is embedded into the foundation or cap beam (illustrated in Fig. 1 for the cap beam connection). Design expressions for this connection have been proposed in previous research (Stephens et al. 2016a). The strength and stiffness of the CFST columns were evaluated using recommendations in the AASHTO Guide Specifications (2015).

3 NUMERICAL MODELLING

3.1 Model Overview

The open source structural analysis software OpenSees was used to conduct the nonlinear dynamic analyses. The model included the columns, cap beam, diaphragms, precast girders, deck, and abutments as illustrated in Fig. 2. Similar OpenSees models have been used to model RC bridges in previous research (Berry and Eberhard 2003; Ranf 2007).

To model the response of the bridge, the models needed to capture the non-linear response of the columns and connections. In contrast to other PBEE evaluations of RC bridges in which the Takeda hysteresis model (Otani 1981) was used to capture column non-linearity (Mander et al. 2007; Tehrani and Mitchell 2012; Tehrani et al. 2014), the columns and connections were modelled using a fibre-based approach. Plasticity along the effective length of the columns was captured using distributed plasticity beam-column elements, while zero-length fibre elements (herein referred to as connection elements) were used to capture local effects at the column-anchorage interface such as bar/tube buckling and strain penetration as indicated in Figure 2. A forced-based formulation was selected for the beam-column and connection elements to improve computational efficiency in terms of convergence and analysis time. Five integration points were used along the length of the columns based on convergence studies

conducted in previous research (Berry and Eberhard 2007; Ranf 2007). Fibre elements with concrete and steel constitutive models were defined at each integration point to define the cross section of the RC and CFST columns. The sections were discretized according to recommendations by Berry and Eberhard (2007) as illustrated in Figure 2. Note that the connection elements were assigned the same geometric section definitions and section discretization as the beam-column elements. The shear and torsional behaviour of the columns were modelled elastically and flexibilities were assigned based on gross section properties. Fixed boundary conditions were applied to the base of each column in the transverse and longitudinal direction of the bridge; soil-structure interaction was not considered in the analysis. The top of the columns were attached to a rigid link which modelled the offset from the top of the column to the centre of mass of the superstructure.

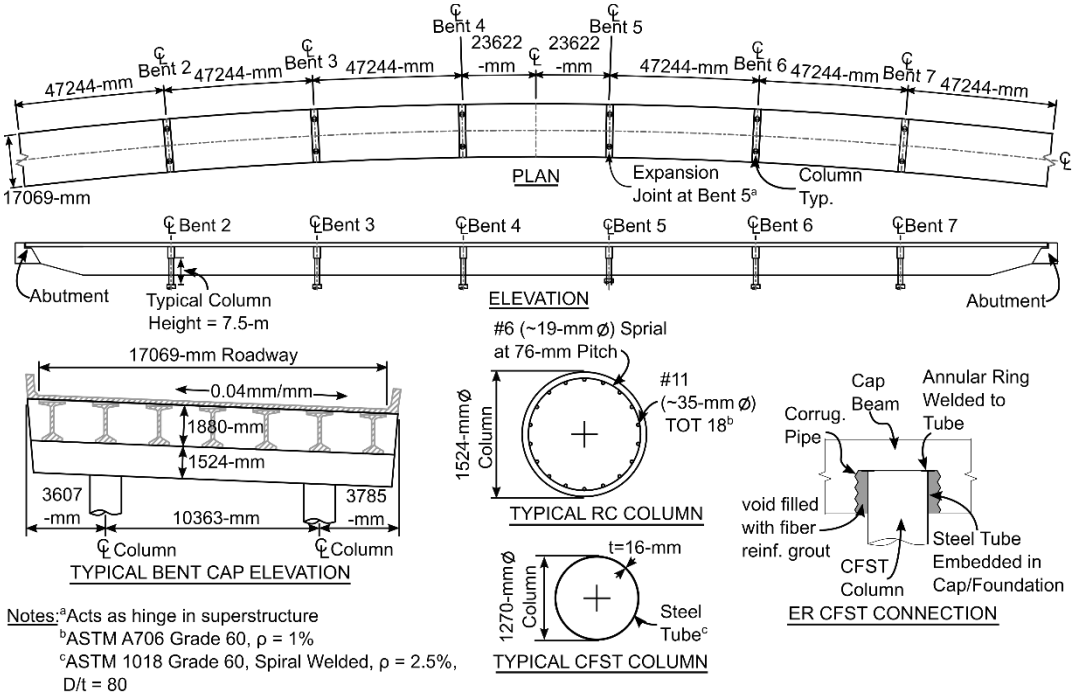

Figure 1. Case Study Structure

All components of the superstructure were idealized using elastic beam-column elements assuming that the structure was capacity designed such that inelastic deformation was isolated to the columns and their connections. In the longitudinal direction, the cross sectional properties of the longitudinal girders, deck, and overlay were aggregated to a single line of elements placed at the centre of mass of the superstructure. In the transverse direction, the cross section properties of the cap beam and diaphragm were aggregated to a single line of elements also located at the centre of mass of the superstructure (illustrated in Figure 3). Mass was lumped at nodes between the elements.

The influence of the abutments was modelled using springs attached to the superstructure at both ends of the bridge as indicated in Fig. 2. The stiffness of the springs was calculated based on recommendations in AASHTO (2015) for the vertical and transverse stiffness of the elastomeric bearing pads between the longitudinal girders and abutment seats.

Orthogonal ground motions were applied to the fixed boundaries for the dynamic analysis using a built-in function in OpenSees as indicated in Fig. 2. Note that the same motion record was applied to each column for each event (i.e. multiple support excitation was not considered).

3.2 **Non-Linear Constitutive Models for Columns**

The influence of strain penetration, tensile yielding, and compression buckling in longitudinal reinforcing (in the case of RC) or steel tube (in the case of CFST) as well as concrete cracking and crushing in the columns were modeled using non-linear constitutive models available in OpenSees. The uniaxial material models used to define the steel and concrete behaviours in RC columns have been used extensively in previous research (e.g. Berry and Eberhard, 2007, Ranf, 2007). Special attention was

given to accurately capturing the response of the ER CFST connection which includes strain penetration in the embedded region of the steel tube as well as local tube buckling near the CFST column to foundation/cap beam interface. The material definitions used to capture these behaviours are described in-detail in reference material (Stephens 2016). The accuracy of the non-linear modeling procedures for the RC and CFST columns were validated using experimental data from column subassembly tests which represent a range of common structural parameters used in highway bridges at the prototype scale (Stephens 2016).

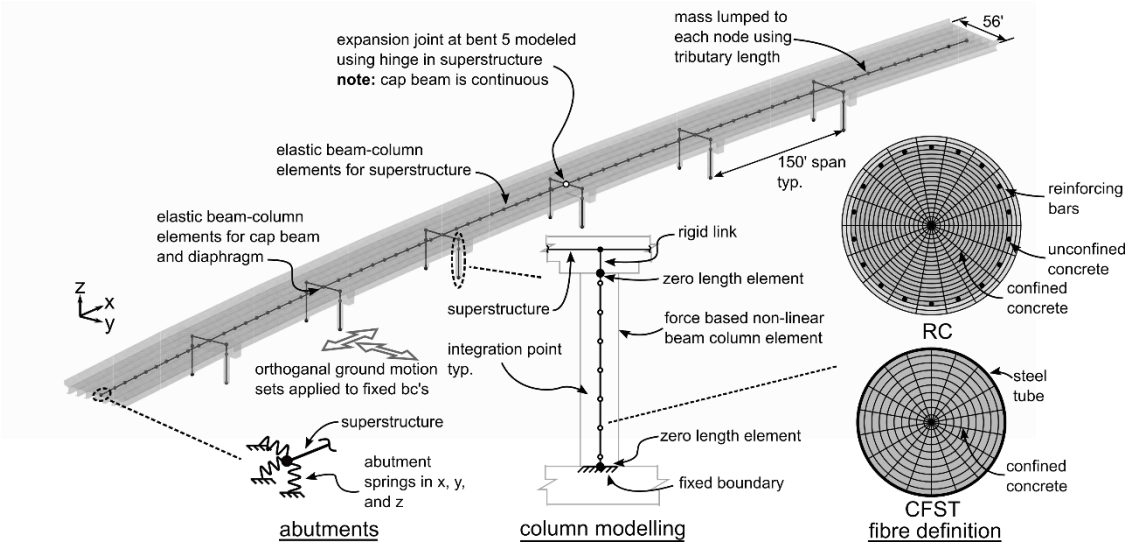

Figure 2. Model Overview

4 QUANTIFICATION OF PERFORMANCE STATES

The damage states of the RC and CFST structures were estimated based on the maximum drifts recorded in the dynamic analysis. Damage in the RC structure was approximated using recommendations from Berry and Eberhard (2003) which estimate drifts at spalling and bar buckling in RC bridge columns from a database of 140 circular RC columns. The damage state of the CFST structure was estimated using a fragility function for the ER CFST connection which estimates the probability of steel tube tearing as a function of the maximum observed drift ratio. The fragility function was developed using an experimental database consisting of 23 large-scale ER CFST connection specimens which represent a range of typical D/t ratios and material properties that would be found in full-scale CFST bridge structures (Stephens 2016; Stephens et al. 2016a).

The performance of the RC and CFST structures were evaluated based on the required post-event repair effort, which in turn was, correlated to the estimated severity of damage. As the superstructure and foundation were assumed to remain elastic in the numerical model, only repair scenarios related to column damage are considered here. Post-event repair scenarios were defined as *No Repair*, *Repair*, *Partial Replace*, and *Collapse/Full Replacement*. Damage corresponding the repair scenarios is summarized in Table 2.

Table 1. Required Repair Effort for RC and CFST Columns

Required Repair Effort	**RC Damage** **Repair Effort**	**CFST Damage** **Repair Effort**
No Repair	Bar Yielding	Tube Yielding/Buckling
Repair	Limited Column Spalling Inject Cracks with Grout	N/A
Partial Replace	Bar Buckling/Fracture Shift Plastic Hinge Region	Steel Tube Tearing Shift Plastic Hinge Region
Collapse/Replace	Drift > 10%	Drift > 10%

5 MULTIPLE SEISMIC HAZARD LEVEL ANALYSIS

5.1 Seismic Hazard Levels

The performance of the RC and CFST bridges were evaluated for a three different seismic hazard levels at the site of the bridge; the response of each bridge was quantified in terms of maximum drift demand and performance states in terms of the required post-event repair required. Thirty-nine crustal ground motions recommended in FEMA P695 (2008) were used in this investigation. Characteristics of the ground motions are available in Stephens (2016). The motions were scaled to meet the target spectrum at the fundamental period (the fundamental periods of the RC and CFST structures were both approximately 1-sec as calculated using an eigenvalue analysis) for all three hazard levels: 10/50 (serviceability level), 7/75 (design level), and 2/50 (MCE) hazard levels.

The target spectra for the 10/50 and 2/50 hazards followed FEMA P750 (2009) recommended provisions using the corresponding USGS mapped spectral acceleration values representative of the different hazards. The target spectra for the 7/75 hazard was developed based on requirements from AASHTO (2015). All of the records were scaled to the fundamental period of the structures such that the mean spectrum did not drop below 70% the target spectra over a period range from 0.2T to 1.5T. The target and mean acceleration spectra for the three hazards are shown in Fig. 3.

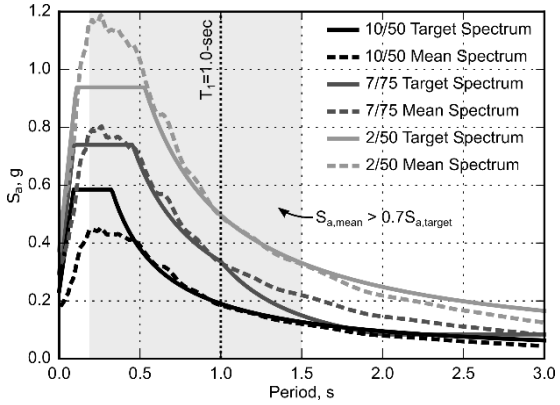

Figure 3. Target Spectra and Corresponding Mean Acceleration Spectra

5.2 Structural Response

The median-maximum recorded drifts for the RC and CFST bridges are summarized in Table 6, while the percentage of motions exceeding the *Repair*, *Partial Replace*, and *Collapse/Full Replacement* limit states for each hazard are shown in Fig. 4. Note that the median-maximum recorded drift was calculated as the median of the maximum drifts observed in any bent for a particular ground motion. In general, the CFST structure performed better than the RC structure in terms of maximum drift levels and required post-event repair. The RC structure exhibited median-maximum drifts of 1.39%, 2.90%, and 3.75% for the 10/50, 7/75, and 2/50 hazards respectively. Although these drifts appear relatively low, over 70% of the motions resulted in at least a *Repair* post event scenario for all seismic hazards as indicated in Fig. 4. The drift threshold for the *Partial Replace* scenario was exceeded in 10% of motions scaled to the design level hazard, and 33% of motions scaled to the MCE level (refer to Fig. 4). The CFST structure exhibited median-maximum drifts of 1.26%, 2.33%, and 2.90% for the 10/50, 7/75, and 2/50 hazards respectively. None of the motions in the serviceability or design level hazards exceeded the threshold of the *No Repair* post event scenario for the CFST structure as indicated in Fig. 4. Further, the *Partial Replace* limit state was exceeded by 10% of the MCE level motions.

Table 2. Mean and Standard Deviation of Maximum Recorded Drifts

	10/50		7/75		2/50	
	$\bar{x}$	σ	$\bar{x}$	σ	$\bar{x}$	σ
RC	1.39	0.19	2.90	0.31	3.75	1.90
CFST	1.26	0.06	2.33	0.11	2.90	1.57
% Difference	9.4	68.4	19.7	64.5	22.7	17.4

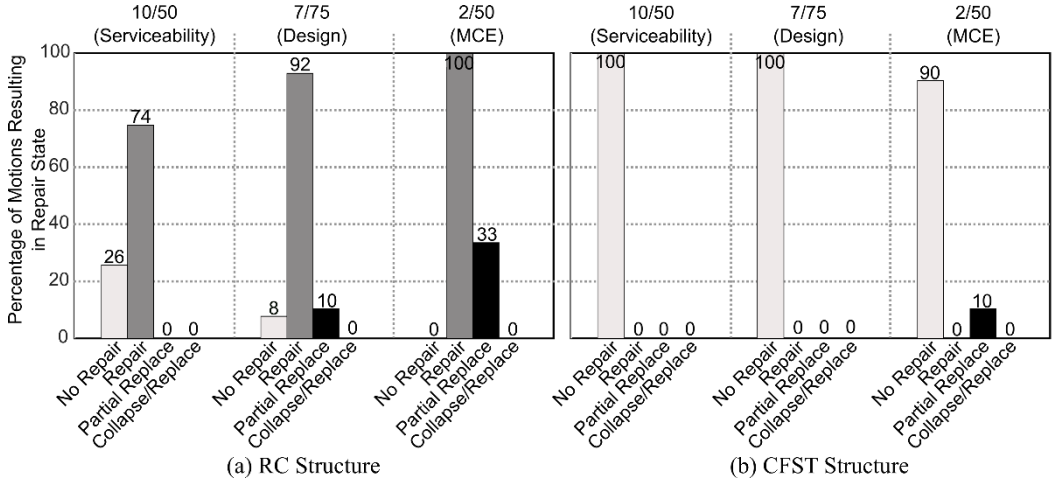

Figure 4. Required Repair Effort for the 10/50 (Serviceability), 7/75 (Design), and 2/50 (MCE) Hazards

6 DAMAGE STATE PROBABILITY USING INCREMENTAL DYNAMIC ANALYSIS

The performance of the RC and CFST case-study structures were additionally evaluated using an IDA in which the structures were subjected to the same suite of ground motions scaled multiple and increasing levels of intensity. The ground motions were individually scaled at the fundamental period of the two structures until at least 50% of the motions resulted in collapse, which has been defined as a maximum drift exceeding 10% drift. This drift limit was selected because experiments show that bridge columns typically achieve this deformation while retaining a reasonable portion of their lateral resistance, but typically do not retain sufficient resistance beyond this limit. IDA curves for the maximum recorded drift are plotted in Fig. 5.

Results from the IDA were used to fit lognormal cumulative distribution functions (CDF) (commonly referred to as fragility functions) for the required post-event repair effort as correlated to the maximum recorded spectral acceleration. The lognormal CDF is defined in Equation 1 where Φ is the Gaussian function, S_a is a particular value of the spectral acceleration, θ_d is the logarithmic mean, and β_d is the logarithmic standard deviation.

$$F_d(S_a) = \Phi\left(\frac{\ln(S_a/\theta_d)}{\beta_d}\right) \quad [1]$$

The performance of the RC and CFST structures were evaluated based on the lognormal CDFs for the *Repair*, *Partial Replace*, and *Collapse/Full Replacement* performance states (defined in Table 2). The empirical and closed-form expressions for the CDFs for each repair-based limit states are illustrated in Fig. 6.

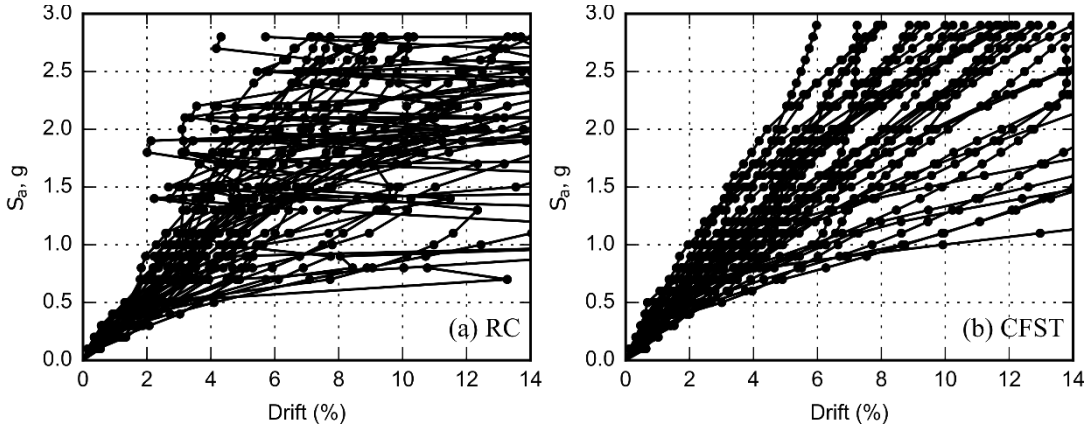

Figure 5. Maximum Recorded Drift from IDA

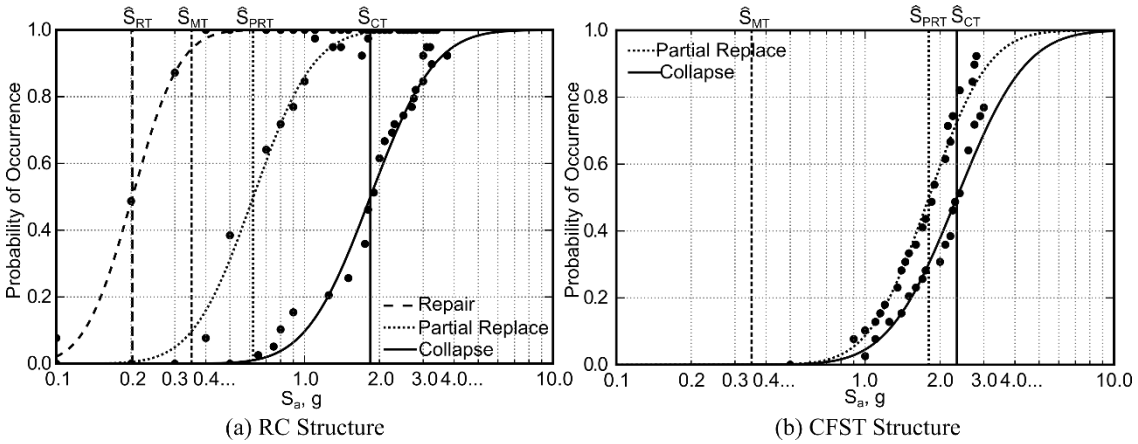

Figure 6. Probability of Required Repair Effort Based on Spectral Acceleration

To provide a direct comparison of the performance of the two structures, the limit states have been expressed in terms of the repair margin ratio (RMR), partial replace margin ratio (PRMR), and collapse margin ratio (CMR) as defined in Equations 12-14, where SMT is the design earthquake spectral acceleration at the period of the structure (the 7/75 target spectrum in Fig. 4), and $\hat{S}_{RT}$, $\hat{S}_{PRT}$, and $\hat{S}_{CT}$ are the median spectral accelerations calculated for the repair, partial replace, and collapse limit states, respectively. The RMR, PRMR, and CMR are summarized in Table 8.

$$RMR = \frac{\hat{S}_{RT}}{\hat{S}_{MT}} \quad [2]$$

$$PRMR = \frac{\hat{S}_{PRT}}{\hat{S}_{MT}} \quad [3]$$

$$CMR = \frac{\hat{S}_{CT}}{\hat{S}_{MT}} \quad [4]$$

The CFST structure had lower values of the RMR, PRMR, and CMR ratios the RC structure in terms, as indicated in Table 7. The CFST structure exhibited significantly larger PRMR and CMR than the RC structure, suggesting the post-event repair effort on the CFST bridge would be less than that required for the RC bridge. An RMR of 0.57 was recorded for the RC structure, indicated a likelihood that repair would be necessary for the design level hazard. Note that no *Repair* limit state exists for the CFST columns (as previously discussed), thus giving the CFST structure a further advantage over the RC system. The advantages of the CFST structure are additionally highlighted by the lognormal CDF curves in Fig. 14, which indicate higher probabilities of repair, partial replacement, and collapse of the RC structure for lower spectral accelerations.

Table 3. Summary of RMR, PRMR, and CMR from IDA

	RMR	PRMR	CMR
RC	0.57	1.71	5.43
CFST	n/a	5.14	6.71
% Difference	n/a	200	24

7 SUMMARY AND CONCLUSIONS

Advanced PBEE tools were used compare the seismic performance of an RC and CFST bridge, including fragility functions, non-linear analyses, and IDAs to evaluate the repair state and collapse potential. The performance of the structures were evaluated based on *Repair*, *Partial Replace*, and *Collapse* limit states correlated to the estimated severity of damage based on the maximum drifts observed in the two structures. Based on the recorded results, the following conclusions were made:

- The performance of the CFST structure exceeded that of the RC structure for all hazards evaluated in the multiple seismic hazard analysis. The maximum recorded drifts in the CFST structure remained below the threshold which would require post-event repair for all motions in the 10/50 and 7/75 hazards, while the RC structure exceeded the threshold for repair for a majority of the ground motions in all hazard levels.

- Results from the IDA indicated that the RC structure has a higher probability of exceeding the *Repair, Partial Replace,* and *Collapse/Full Replacement* limit states than the CFST structure for lower spectral accelerations.
- CFST is an economical and resilient alternative to RC bridge columns for use in seismic regions.

8 REFERENCES

AASHTO. (2015). "AASHTO Guide Specifications for LRFD Seismic Bridge Design with 2012, 2014, and 2015 Interim Revisions." American Association of State Highway and Transportation Official, Washington, DC.

Berry and Eberhard, M.P. & Eberhard, M.O. (2003). "Performance Models for Flexural Damage in Reinforced Concrete Columns." Report for the Pacific Earthquake Engineering Research Centre, Report Number 2003/18.

FEMA P695. (2008). "Quantification of Building Seismic Performance Factors FEMA P695 ATC-63 Project Report, Federal Emergency Management Agency, Washington, D.C.

FEMA P750. (2009). "NEHRP Recommended Seismic Provisions for New Buildings and Other Structures." FEMA P750/2009 Edition: Provisions, Federal Emergency Management Agency, Washington, D.C.

Lehman, D.E., Elkin, S., Nacamuli A. & Moehle, J.P. (2001). "Repair of Earthquake-damaged Bridge Columns", ACI Structural Journal, 98(2).

Lehman, D.E. & Roeder, C.W. (2012). Foundation Connection for Circular Concrete Filled Tubes, *Journal of Constructional Steel Research,* DOI: 10.1016/j.jcsr.2012.07.001.

Mander, J.B., Dhakal, R.P. & Mashiko, N. (2007). and Solberg, K.M., "Incremental Dynamic Analysis Applied to Seismic Financial Risk Assessment of Bridges", Journal of Engineering Structures, DOI: 10.1016/j.engstruct.2006.12.015.

NZ Transport. (2016). "Bridge Manual SP/M/022." Third Edition. New Zealand Transport Agency. Wellington, NZ.

Otani, S. (1981). "Hysteresis Model of Reinforced Concrete for Earthquake Response Analysis", Journal of the Faculty of Engineering, University of Tokyo, Series B XXXVI-11:2, 407-441.

Ranf, R.T. (2007). "Model Selection for Performance Based Earthquake Engineering of Bridges." PhD Dissertation, University of Washington.

Stephens, M.T. (2016). Design Expressions and Dynamic Evaluation of CFST Bridges Subjected to Seismic Hazards, *Ph.D. Dissertation.* University of Washington.

Stephens, M.T., Lehman, D.E. & Roeder, C.W. (2016a). "Design of CFST Foundation/Column-to-Cap Beam Connections for Moderate and High Seismic Regions", Journal of Engineering Structures, DOI: 10.1016/j.engstruct.2016.05.023.

Stephens, M.T., Berg, L.M., Lehman, D.E. & Roeder, C.W. (2016b). "Seismic CFST Column-to-Precast Cap Beam Connections for Accelerated Bridge Construction", ASCE Journal of Structural Engineering, DOI: 10.1061/(ASCE)ST.1943-541X.0001505.

Tehrani, P. & Mitchell, D. (2012). "Seismic Performance Assessment of Bridges in Montreal Using Incremental Dynamic Analysis", Proceedings of the 15th World Conference on Earthquake Engineering, Lisbon Portugal.

Tehrani, P., Goda, K., Mitchell, D., Atkinson, G.M. & Chouinard, L.E. (2014). "Seismic Response Prediction of Bridges Using Incremental Dynamic Analysis with Subduction Zone and Crustal Ground Motion Records", Proceedings of the Tenth U.S. National Conference on Earthquake Engineering, Anchorage Alaska.